Tethys
Journal of Mediterranean Meteorology & Climatology

Tethys 2023, **20**, 1–20
www.tethys.cat
ISSN-1697-1523
eISSN-1139-3394
DOI:10.3369/tethys.2023.20.01
Journal edited by **ACAM**

A Comparative Performance Study of WRF, COSMO and ICON Atmospheric Models for the Italian Peninsula at Very High Resolution

I. Manco[1,2], C. De Lucia[3], F. Repola[1], G. Fedele[1] and P. Mercogliano[1]

[1]Regional Models and Geo-Hydrological Impacts Division, Centro Euro-Mediterraneo sui Cambiamenti Climatici, 81100 Caserta, Italy.
[2]Università degli Studi di Bologna, Dipartimento di Fisica e Astronomia, Bologna, Italy.
[3]Centro Italiano Ricerche Aerospaziali (CIRA), Via Maiorise, 81043 Capua, CE, Italy.

Received: 23-XI-2022 – Accepted: 20-VI-2023 – **Original version**

Correspondence to: ilenia.manco@cmcc.it

Abstract

This study seeks to estimate the precision of three different high-resolution atmospheric models in the simulation of two sets of short-term weather forecasts for a duration of two-weeks for the Italian Peninsula. The following models were used: WRF (Weather Research and Forecasting Model), COSMO (Consortium for Small-scale Modelling) and ICON (Icosahedral Nonhydrostatic Model). The capability of these weather forecasting systems has been evaluated using their optimum-configurations, which were obtained from a tuning procedure at a spatial resolution of about 2 km over Italy.
The models share the same forcings given by the Integrated Forecasting System (IFS) analyses provided by the European Centre for Medium-Range Weather Forecasts (ECMWF) with a grid-point distance between neighbouring points of approximately 0.081° (∼9 km). This study was performed over two periods: from 01/01/2019 to 15/01/2019 and from 16/08/2020 to 30/08/2020. These periods were chosen to characterise the models' performance over the winter and summer seasons respectively. The precision of these weather forecasting systems were evaluated by taking their best-configurations, which were obtained from a tuning procedure at a spatial resolution of 0.018° (∼2 km) over the domain specified. The ERA5-Land reanalysis, which was provided by the Copernicus Climate Change Service (C3S) and the gridded SCIA observed data (SCIA - Sistema nazionale per la raccolta, elaborazione e diffusione di dati Climatologici di Interesse Ambientale). The results for each model reveal that the variables analysed here are all consistent with respect to those observed, as they capture the main features that characterise the summer and winter weather conditions investigated here. Those differences observed among the models may be related to the complex parameterization schemes used in WRF, COSMO, and ICON, that could affect the models' performance.

Key words: Numerical Weather Prediction, WRF-COSMO-ICON, high-resolution modeling, dynamical downscaling

1 Introduction

The Italian Peninsula possesses a highly complex climate variability, one that is led by several factors including complex topography, latitudinal extension, interaction with the Mediterranean Sea, continental and oceanic influences, and the marked impact of climate change (Silvestri et al., 2022).

High climate spatial variability over Italy has motivated researchers to investigate atmospheric processes at higher spatial scale resolutions, using different Limited Area Models (LAM), that are essential for resolving processes at a finer resolution scale and for providing accurate weather forecasts within a short time range, and without the computational costs that characterise global climate models (GCMs). In

this regard, this research aims to investigate the capabilities of three high-resolution atmospheric models in simulating short-term atmospheric variability over Italy for two periods: from 01/01/2019 to 15/01/2019 and from 16/08/2020 to 30/08/2020. These periods were chosen as they are characterised by meteorological phenomena that are linked to high-level local atmospheric impacts: the winter period chosen for 2019 is one dominated by strong winds, while August 2020 is characterised by high warm temperatures and intense precipitation over Italy. Furthermore, the 2 km resolution chosen for the simulations allows us to solve the processes at a convection permitting scale in an explicit manner.

The following three Numerical Weather Prediction (NWP) models at a 2 km horizontal resolution are investigated here: WRF (Weather Research and Forecasting Model; Skamarock et al. (2019)), COSMO (Consortium for Small scale Modelling; Steppeler et al. (2003) and Doms et al. (2011)) and ICON (Icosahedral Nonhydrostatic).

Previous multi-model studies already sought to investigate performance in terms of reproducing weather patterns at different scales. These revealed (Mulovhedzi et al., 2021; Mugume et al., 2018; Caldas-Alvarez et al., 2022) deficits in reproducing high-level local scale features, due to deep-convection events, which are often not solved, even when using ensemble-member configurations (Heppelmann et al., 2017). In this respect, many studies (e.g., Mugume et al. (2018); Caldas-Alvarez et al. (2022)), emphasize the importance of horizontal resolution in the representation of local-scale precipitation patterns. Mugume et al. (2018), for example, when comparing the performance of two different models, WRF and COSMO at a 7 km resolution over the tropics, suggests that the poor performance of the models in reproducing deep-convection processes, may be associated with the use of coarse-resolution. Many studies, such as Caldas-Alvarez et al. (2022), have only investigated the ability of the models to reproduce and predict local extreme events over small areas and short time periods at a high resolution due to the high computational demands of long-term simulations.

Another key feature, and one that plays a fundamental role in the NWP Models are model physics parameterizations. In greater detail, Heppelmann et al. (2017), when investigating the mean diurnal cycle for wind over Europe, using COSMO and ICON models at 6.5 km and 7 km, respectively, found that the deficiencies of these models may be attributable to the inherent properties of model physics. It is therefore increasingly important to perform high resolution simulations, downstream of a sensitivity analysis of the physical schemes in order to obtain realistic results.

In this framework, the main purpose of this study is to investigate reliable configurations for WRF, COSMO and ICON at a convection-permitting scale ($\sim$2 km horizontal resolution) over the Italian Peninsula, a land mass that is characterized by a complex orography and air-sea interaction processes. In specific terms, the ability to capture the patterns of two typical weather conditions that characterise the Italian Peninsula were investigated: cold temperatures and strong winds in winter (2019) and intense convection in summer (2020). Each simulation was of a two-week duration.

The results obtained in this study are valid for the weather conditions analysed, and should not be construed as general conclusions for other meteorological events that characterize the Italian Peninsula. A detailed discussion on each model is provided in Section 2, where their main characteristics and the sensitivity analysis performed to identify the respective optimum configurations for the selected test cases are examined. Within this framework, this investigation provides an overview of the main strengths and weaknesses of each model, while providing insights for future modelling applications.

2 Data and Methods

In this section, the modelling configurations and the observational data used to validate the model results are discussed and the diagnostics used in this research project are also presented.

2.1 Models and Simulations: the Set-Up used

The atmospheric forcing used was the Integrated Forecasting System (IFS) with analyses provided by the European Centre for Medium-Range Weather Forecasts (ECMWF), with a grid-point distance between neighbouring points of approximately 9 km. The simulations were conducted in a single run of 15 days and the lateral boundary conditions for each model were refreshed every 6 hours. A preliminary sensitivity analysis was performed on each model in order to define their optimum configurations. The main features of the configurations of each model are summarised in Table 1. Details regarding the models' main characteristics and best configurations are discussed below.

2.1.1 The WRF Model

The Weather Research and Forecasting Model (Skamarock et al., 2019) development originates from a collaborative partnership that began in the second half of the 1990s between the U.S. National Center for Atmospheric Research (NCAR), the U.S. National Oceanic and Atmospheric Administration, the U.S. Air Force, the U.S. Naval Research Laboratory, the University of Oklahoma and the Federal Aviation Administration (FAA). It is totally compressible and is not hydrostatic (it has a hydrostatic option in run-time). During this research work its most-recent version at the time of writing V4.2.1 (22 July 2020) was used, this is one that is characterised by significant improvements when compared to previous versions. The two-dimensional grid adopted in horizontal domain discretization is provided by the Arakawa Staggered C-grid, while the time-integration scheme used in

Table 1: WRF, COSMO and ICON Model Set-up

Model	Forcing	Grid Type	Horizontal Resolution	Horizontal Discretization	Time Step	Vertical Coordinates
WRF	IFS (ECWMF) 0.075º	Regular Lat-Lon (Lambert)	2 km	Arakawa C-grid	12 s	sigma pressure (60 vertical levels)
COSMO	IFS (ECMWF) 0.075º	Rotated grid	2 km	Arakawa C-grid	20 s	60 vertical levels
ICON	IFS (ECMWF) 0.075º	The unstructured icosahedral-triangular grid	2 km	Arakawa C-grid	24 s	65 vertical levels

Table 1 cont.

Model	Temporal Integration Scheme	Spatial Differentiation Scheme
WRF	Runge-Kutta scheme of 3º order	6th order centre differencing
COSMO	Runge-Kutta scheme of 3º order	Finite differences
ICON	Two-time level predictor-corrector time stepping scheme	Mixture of finite volume / finite difference discretization

the ARW resolver is the Runge-Kutta (RK) type for low frequency, (meteorologically-significant) motions, with an accuracy of the third order for linear equations and the second order for nonlinear equations (e.g., Laprise (1992); Skamarock et al. (2019)). The WRF model is characterised in this version by the use of a hybrid vertical coordinate (sigma-pressure), as reported in Park et al. (2019). Sixty levels are equally distributed from 0 hPa to 1000 hPa.

The configuration adopted to enable comparison with the other two atmospheric models discussed here comes from a previously-held, and carefully-conducted sensitivity analysis that sought to define the best WRF configuration for the domain of specific interest, by varying different physical patterns, such as the PBL and Microphysics scheme (Kim et al., 2013), and the adopted cartographic projection (Lambert and Mercator), as detailed in Table A1 in Appendix A. The sensitivity experiments share the same horizontal resolution (2 km) and the same forcing (ECMWF analyses at approximately 9 km resolution). This sensitivity analysis allowed us to identify Sim9 as the best model configuration, by evaluating the model temperature and precipitation fields against observations (not shown here). The statistical indicators; MAE (mean absolute error), RMSE (root mean square error), MBIAS (mean bias), IoA (Index of Agreements) and Taylor Diagrams were used in the validation process. A significant improvement in performance was noted in the use of the Planetary Boundary Layer "YSU" scheme, which reproduces both the temperature and precipitation ranges in a more reliable manner. In terms of microphysics schemes, the "Morrison 2-moment scheme" provided the best choice to correctly reproduce the precipitation field. Moreover, less distortions occur using a Lambert cartographic projection rather than a Mercator projection. The Monin-Obukhov scheme (Janjic Eta) was used for all simulations in order to parameterize the surface layer.

2.1.2 The COSMO Model

The COSMO model (Steppeler et al., 2003; Doms et al., 2011) is a nonhydrostatic limited-area atmospheric prediction model that is developed and maintained by the COSMO consortium (Cosmo Public Area available online: http://www.cosmo-model.org/). Several options for a two time-level second and third order Runge–Kutta split-explicit scheme are available (Baldauf et al., 2011). The vertical integration is performed on 60 levels from 100 hPa to 1000 hPa. The model implements the next-generation TKE-based surface-layer transfer scheme (Buzzi, 2008; Doms et al., 2011). The COSMO 5.05 version features a new ICON-based physics that involves a different turbulence scheme (Schättler et al., 2018). The physical parameterization schemes include the multi-layer land surface model TERRA (Steppeler et al., 2003; Schulz et al., 2015). Urban–atmosphere interactions are taken into account with the urban canopy model Terra-Urb (Wouters et al., 2015, 2016). The urban scheme considers urban physics in terms of surface energy and moisture exchanges, including the influence of street-canyon geometry. The Terra-Urb scheme provides corrections for the surface parameters (roughness length, albedo, emissivity, heat capacity, etc.) within the framework of the TERRA module, using the semi-empirical urban canopy dependencies. The configuration adopted in this paper comes from a sensitivity analysis that was performed by Garbero et al. (2021).

2.1.3 The ICON Model

In 2018 the COSMO consortium began the migration process from the COSMO-LM (Steppeler et al., 2003) to the ICON-LAM (ICON Limited Area Model), which was to be implemented as the subsequent operational model. The Icosahedral Nonhydrostatic Model (ICON) was developed by the German Weather Service (DWD) and the Max

Planck Institute for Meteorology (MPI-M; Zängl et al. (2015)) in order to build a next generation of NWP models that guarantee better conservation properties, improved scalability on parallel high-performance computers, and the possibility of performing static mesh refinement. An icosahedral-triangular Arakawa C-grid was used. The set of governing equations was based on the fully compressible non-hydrostatic system for the representation of a two-component system (dry air and water in all the three phases). There were 60 vertical levels for the model that were uniformly distributed from 50 hPa to 1000 hPa.

In this paper, using the ICON version 2.6.2.2 the model configuration was the result of a sensitivity analysis that was performed on the Italian Peninsula with a spatial resolution of approximately 2 km, as discussed in De Lucia et al. (2022) and in Table A2 in Appendix A.

2.2 The Observational Dataset

In order to assess the ability of the models to reproduce the observed fields, two different datasets were analysed in this study: ERA5-Land (Muñoz Sabater et al., 2019; Muñoz-Sabater et al., 2021) and SCIA (Desiato et al., 2007).

ERA5-Land is a reanalysis dataset that has provided a wide set of atmospheric-land variables from January 1950 to the present day, at high temporal (hourly) and spatial (0.1° x 0.1°, approximately 9 km) scales over the entire globe. This dataset therefore allows us to investigate the atmospheric processes at enhanced temporal and spatial scales when compared to other reanalyses. The following variables have been used to assess the models' skills: the mean, minimum and maximum temperature (t_{mean}, t_{min} and t_{max}, respectively), the mean wind speed W_{10m}, and the daily cumulative precipitation Tot_{prec}.

In addition to ERA5-Land, the SCIA dataset has been used in order to emphasise the ability of the models to reproduce the temperature fields at a higher spatial resolution. The SCIA is an observational dataset formed by hundreds of stations that cover the entire Italian Peninsula (free access at http://www.scia.isprambiente.it/wwwrootscia/help_eng.html). In this study, we used the daily gridded data product, which covers a period from January 1961 to December 2020 on a regular grid of 5 km resolution for t_{min} and t_{max} respectively, and 10 km for the Tot_{prec}. The gridded t_{mean} and W_{10m} fields are not available for the SCIA dataset and therefore the corresponding simulated fields will be evaluated against ERA5-Land only.

2.3 Methodology

This research aims to assess the capabilities of the above-mentioned models for short-term weather forecasts of the Italian Peninsula. To this end the following simulated fields were analysed against the observations: the daily cumulative precipitation field, the minimum, average and maximum surface temperature and, finally, wind speed at 10-metres. An objective method of comparison was then proposed, which makes use of the following diagnostics: Time-mean fields, Probability Density Function (PDFs) and Taylor Diagrams.

The PDF represents the probability range as a function of the magnitude value examined and it provides an immediate representation of the data distribution, while, the Taylor diagrams provide a graphical framework that allows a comparison to be made among models S and reference data O in terms of Root Mean Square Error ($RMSE$), correlation coefficient (RHO), and the standard deviation (σ) of their variances.

3 Results

The main results are detailed in this section. The best-model configurations for WRF, COSMO and ICON have been evaluated against two observational datasets: ERA5-Land and SCIA, in order to highlight their ability to simulate the observed atmospheric fields: t_{min}, t_{mean}, t_{max}, Tot_{prec} and W_{10m} using several diagnostic methods. This study aims to emphasise the main strengths and weaknesses of each model by means of this approach.

3.1 Temperature

The time-mean temperature field and the short-term weather variability over Italy in the reference period are discussed here, with an evaluation of the models at a resolution of 2 km, against ERA5-Land and SCIA (at resolutions of 9 km and 5 km respectively). Resolution-based differences emerge in Fig. 1, with evident signatures of the models' abilities to resolve processes at finer resolutions. In this respect, SCIA allows an improved investigation of consistency of the simulated fields at these scales when compared to ERA5-Land.

Visual inspection reveals that WRF, COSMO and ICON agree with the observed fields. The models showed the same range of values and pattern distribution in 2019 (Fig. 1 a,b,c,d,e) and 2020 (Fig. 1 f,g,h,i,l) as observed in SCIA and ERA5-Land. Lower maximum temperature values were found along the Alps and Apennines in both periods, with negative temperatures exceeding -5°C in 2019, while values lower than 25°C were found on the Apennines and Alps, with the lowest values at around 10°C. Higher temperatures characterise the Italian coasts, reaching values around 15°C in winter and ∼35°C in summer. High t_{max} were also found in 2020 in inland areas such as in Emilia Romagna and the Basilicata Region.

As with the t_{max} fields, the t_{min} simulated fields were also consistent with the observations (Fig. 2). In 2019, SCIA and ERA5-Land showed different patterns in Northern Italy that probably emerged due to the finer resolution in SCIA. In 2019, the minimum temperature appears to have been better captured in ICON than by the other models, which despite accurately reproducing the range of values and the main patterns over Italy, overestimated temperatures in Northern

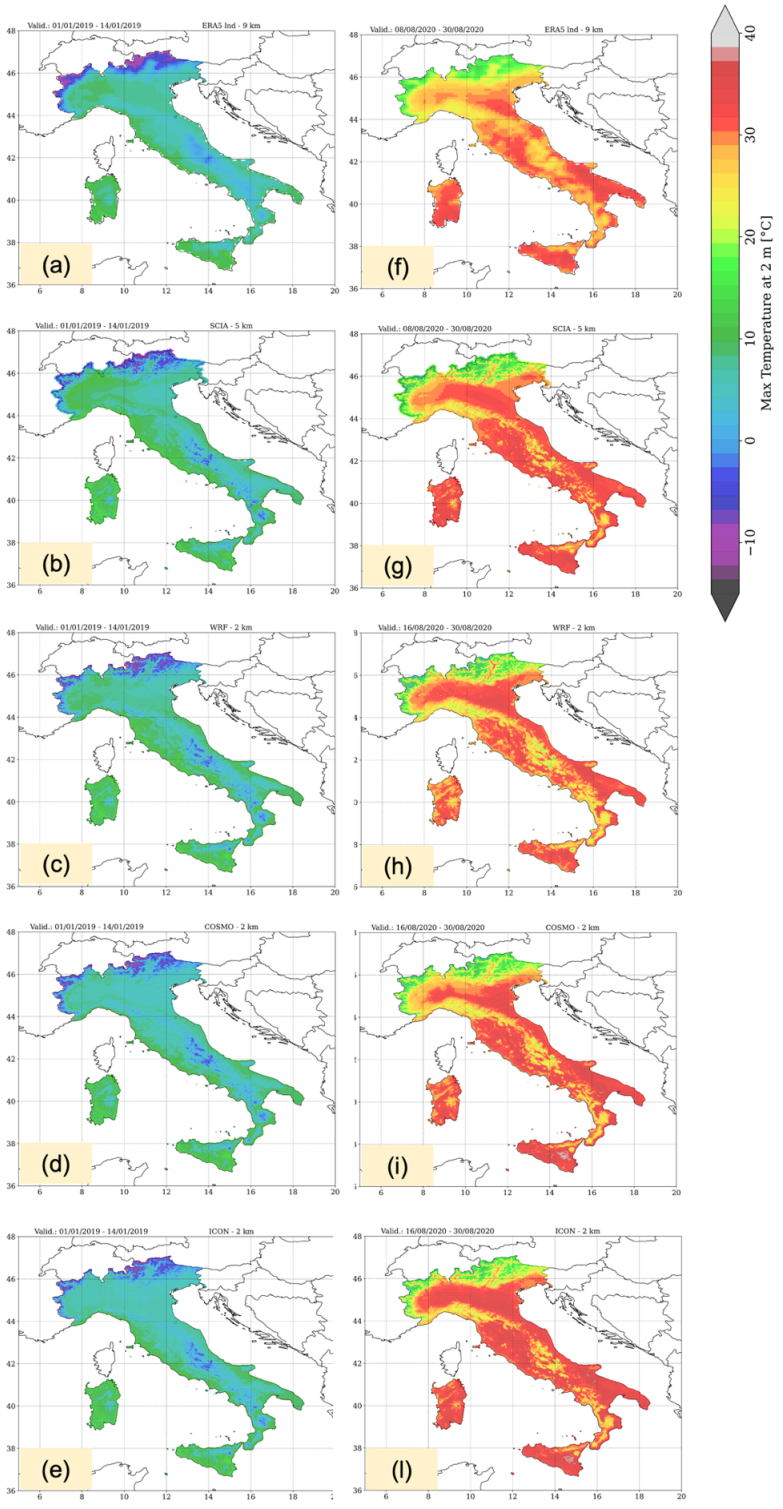

Figure 1: Map of Time-mean Maximum Temperature at 2m for ERA5-Land (a,f), SCIA (b,g), WRF (c,h), COSMO (d,i) and ICON (e,l).

Italy, especially in Emilia Romagna and Tuscany. The lowest temperatures were found in the Alps and the Central Apennines and agreed with the observations in each model, reaching minimum temperature whose lowest peaks were below -10°C in 2019 and ∼10°C in 2020. The highest t_{min} values were seen on the coasts, with values exceeding ∼22°C along the Adriatic shoreline. WRF and ICON overestimated the highest peaks of t_{min}, while COSMO gave a better reproduction of the observed field in 2020.

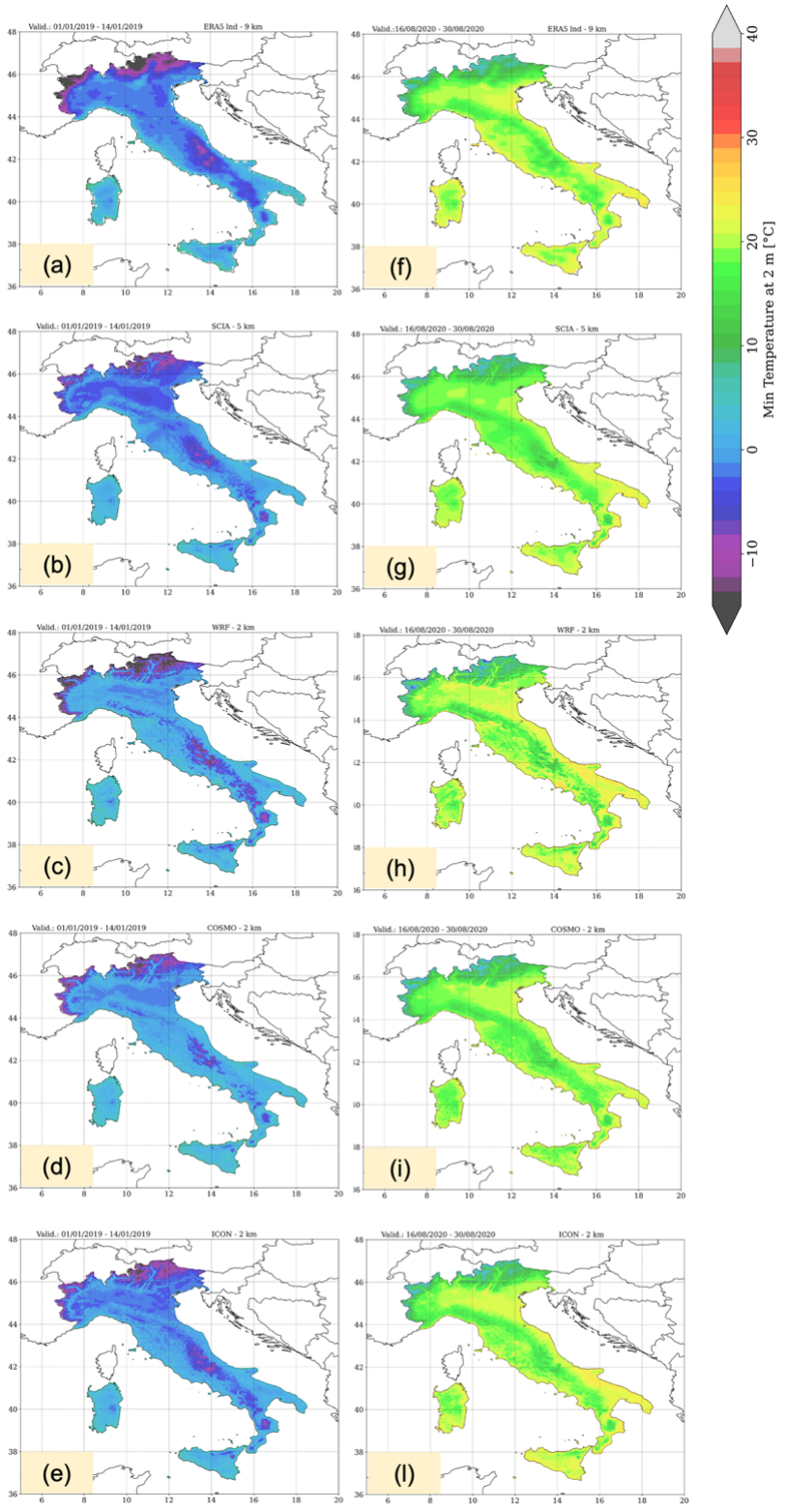

Figure 2: Map of Time-mean Minimum Temperature at 2m for ERA5-Land (a,f), SCIA (b,g), WRF (c,h), COSMO (d,i) and ICON (e,l).

The mean temperature field simulated by the three models was evaluated against that observed in the ERA5-Land data in Fig. 3. SCIA was not included in this analysis, as it did not provide the t_{mean} field product. The range of values was comparable, among the datasets, to a higher coherence between ERA5-Land and COSMO, when compared to WRF

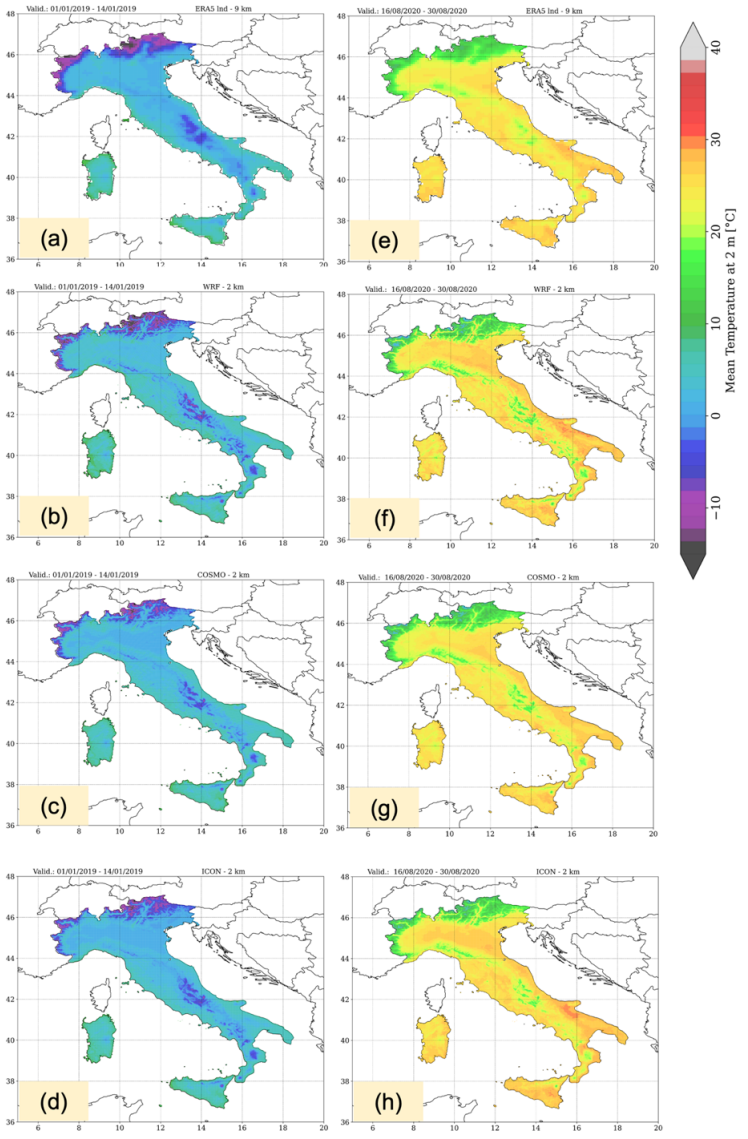

Figure 3: Map of Time-mean Average Temperature at 2m for ERA5-Land (a,e), WRF (b,f), COSMO (c,g) and ICON (d,h).

and ICON, that both overestimated the mean temperatures.

After this preliminary discussion, more robust statements are provided below, analysing the above-mentioned variables in terms of PDFs and Taylor Diagrams. Fig. 4 and Fig. 5 show the PDFs for t_{max}, t_{min} and for the t_{mean} with respect to ERA5-Land and SCIA in 2019 and 2020, respectively). When comparing Fig. 4 (a) and Fig. 4 (d), small differences between ERA5-Land and SCIA emerged for 2019 in t_{max}: the main mode in ERA5-Land is centred around 7°C, while in SCIA it shifts towards higher values (∼9°C), with a frequency of appearance that is higher than the correspondent mode in ERA5-Land. Furthermore, ERA5-Land, when compared to SCIA, tends to overestimate the number of episodes with temperatures below 7°C and to underestimate the number of episodes with temperatures above 9°C. The PDF model that matches that observed the closest belongs to WRF. This latter model has same range of values, and it skews towards higher values in the same ways, as in the observations, as well as in the similar probability of occurrence as captured by the SCIA dataset, while, COSMO and ICON accurately capture the range of temperature values but overestimate the number of events with t_{max} between 3 to 7ºC . A hint of bimodality is captured in ICON, which is not present in the other datasets. For 2020 (Fig. 5), the models accurately simulate the ERA5-Land PDF for values lower than 22°C, but underestimate the number of episodes with t_{max} between 22 to 32ºC and overestimate the probability for the events with temperatures higher than ∼28, 32 and 32°C in WRF, COSMO and ICON respectively (Fig. 5 a). However, when comparing the PDFs model for t_{max} with

the respective PDF found in SCIA (Fig. 5 d), the models better resemble the PDF observed: every model overestimated the probability of events with temperatures higher than 37°C, while underestimating probability of occurrence in the range: 28 to 32ºC. The model which better matches the observed PDF is WRF.

For 2019, the PDFs for t_{min} ERA5-Land and SCIA (Fig. 4 b, e) still present slight differences, i.e. a higher probability peak in ERA5-Land and a bimodal hint in SCIA which is less pronounced in ERA5-Land. By way of contrast, the range of values and the skewness are shared by the two observational datasets. As there are no broad differences between the two-reference data, the models' shift with respect to the observations is similar. COSMO and ICON fit the observed range of values, while in WRF, few episodes with temperature lower than -20°C are also found. A clear t_{min} bimodality is simulated by ICON, which is not present in the other models, however this characteristic is hinted at in the observations. COSMO, WRF and ICON overestimated the number of events with temperatures between 0 and 5ºC in 2019.

When investigating the same variable for the 2020 reference period, a stronger consistency between the models and the observation is found in terms of PDFs (Fig. 5 b, e). On a first comparison ERA5-Land and SCIA, revealed the same range of values, and a similar skewness and kurtosis. The main mode in ERA5-Land centres around 20°C, while in SCIA it is found at around ∼18°C with a higher probability of occurrence. WRF and ICON slightly overestimated events with t_{min} higher than 22°C, underestimating the frequency of occurrence for temperature in the range of 15 to 22ºC. COSMO however slightly underestimated those events with temperatures over 22°C, when compared to ERA5-Land, favouring a t_{min} centred around the observed peaks. Making the same comparison with SCIA, COSMO overlapped the observed distribution better, highlighting better performances with respect to the remaining models for t_{min}.

In Fig. 4 (c) and Fig. 5(c) (2019 and 2020 respectively) the t_{mean} is evaluated against ERA5-Land alone, since the gridded product for this variable is not provided for SCIA, as has mentioned above in Section 2. With respect to 2019, the t_{mean} observed PDF has a peak centred around ∼3°C and covers a temperature range between -15 to 14ºC. The models also cover the observed range but overestimated episodes with temperatures of 3 to 7ºC. The ICON PDF better follows its observed counterpart, revealing a hint of bimodality. With regard to 2020, the models matched the observed PDF, with a higher consistency between COSMO and ERA5-Land when compared to the others. Nevertheless, differences were found between the modelled and the observed PDFs, as WRF, COSMO and ICON reproduced the observed variability well.

A more robust and quantitative measure of the models' capabilities is provided by the Taylor diagrams, which show their correlation in a compact view. The root-mean-square difference and the standard deviation of their variances were evaluated against the reference data. Fig. 6 shows these measures for 2019 and 2020 for the t_{max} (Fig. 6 a,b,c,d), t_{min} (Fig. 6 e,f,g,h) with respect to ERA5 and SCIA and for the t_{mean} (Fig. 6 i,l) with respect to ERA5. The graphs clearly show more than a correlation of more than 90% between the 3 models and the two observational datasets for each variable.

The Taylor diagrams shown in Fig. 6 are discussed below. For 2019, the models estimated a variability with correlations exceeding a value of 95% (Fig. 6 a). ICON reached a value of 99% RHO , while COSMO correlation with ERA5 data stood at approximately 98% while the figure for WRF was 97%. Each model exhibits a standard deviation of its variability which is very close to the observed model (1.9°C). The model that matches the observed σ the closest is COSMO (1.9°C), followed by WRF (1.92°C) and ICON (2.1°C). Finally, the $RMSE$ gives values between 0.3 and 0.5ºC, thus highlighting that the simulations are highly consistent with ERA5-Land. In 2020 (Fig. 6 b), RHO is about 95% in the models (94, 95, 96% in ICON, COSMO and WRF respectively). The standard deviation of the models is very close to the referenced model (1.1, 1.2, 1.5°C in ICON, WRF and COSMO respectively, against 1.4 in ERA5-Land), while the $RMSE$ is below 0.6°C. The model which better matches ERA5-Land for t_{max} is WRF, in terms of both RHO, $RMSE$ and σ. While, considering SCIA as reference dataset, the model that better represents the t_{max} for 2019 was ICON, while for 2020, WRF was the better model (no significant changes were found when compared to Fig. 6 b). This of course highlights the differences between the two observational datasets: in SCIA the standard deviation is higher than in ERA5-Land (2.1 and 1.9°C respectively). Moreover, the $RMSE$ between the models and the reference model increased using SCIA (the mean value between the models' $RMSE$ shifts from 0.30 to 0.55°C). The use of a specific observational dataset with respect to others may therefore influence the evaluation of their capabilities.

The t_{min} in the models was evaluated against ERA5 in Fig. 6 (e) and (f) and SCIA in Fig. 6 (g) and (h). As already observed for t_{max}, RHO for 2019 reached values of around 95% in each model (Fig. 6 e). The models have σ close the reference model (1, 1.42, 1.58°C in COSMO, WRF and ICON respectively, against 1.4°C in ERA5-Land). The $RMSE$ was about 0.45°C in each simulation. Therefore, the three models accurately reproduce the t_{min} in 2019, however WRF better models the variability of the t_{min} . For 2020 (Fig. 6 f), RHO reached the lowest values of Fig. 6 (82, 85, 94% in WRF, ICON and COSMO respectively), the $RMSE$ increased, reaching higher values in WRF (0.48°C), followed by ICON (0.4°C) and COSMO (0.24°C). The σ were close to the reference model (0.7, 0.75, 0.8°C in COSMO, ICON and WRF, compared to 0.75°C in ERA5-Land. The model which performed better in terms of t_{min} in 2020 with respect to ERA5-Land is COSMO. When evaluating the simulated t_{min} with the SCIA model (Fig. 6 g, h), different results were found with respect to ERA5-Land. This again means that

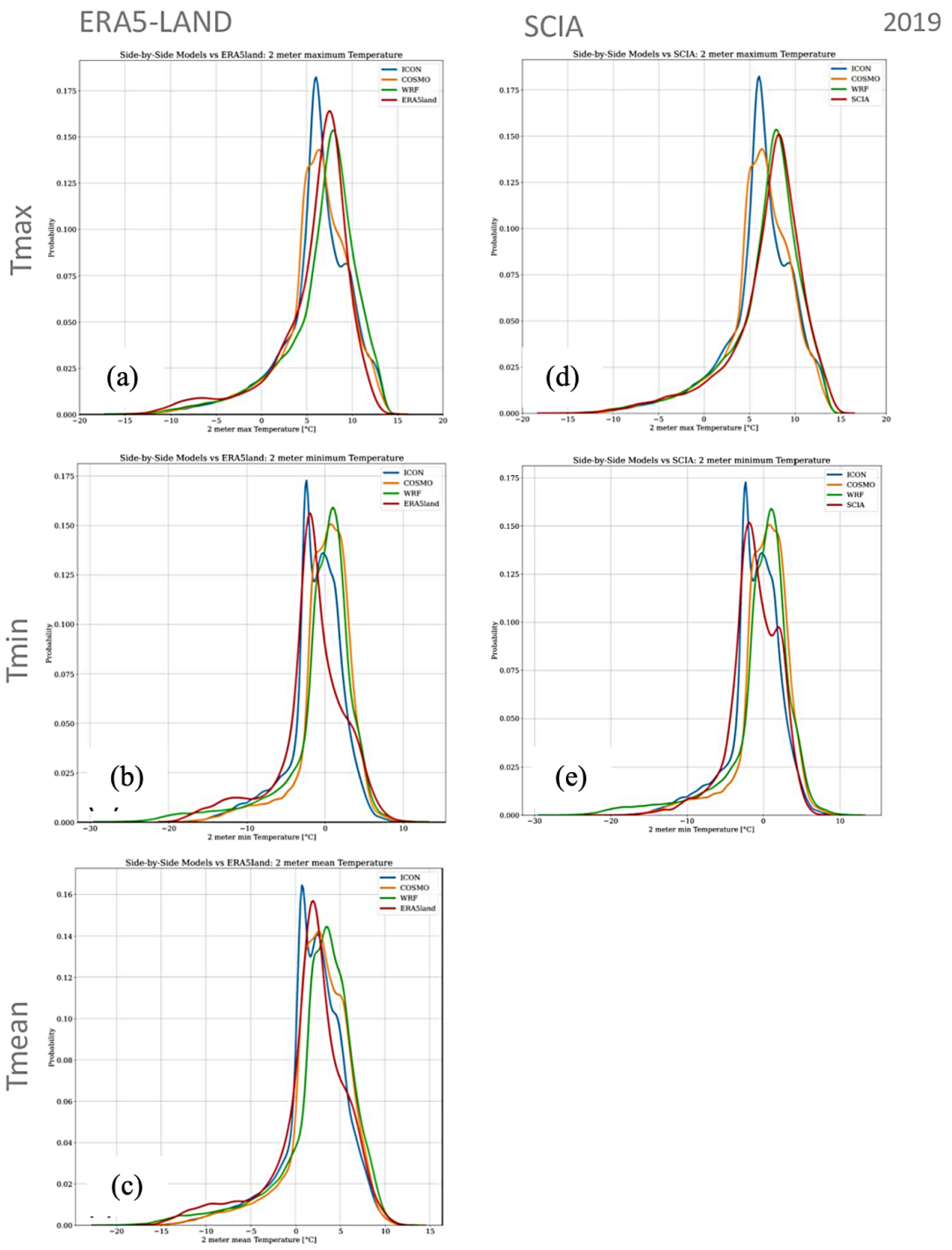

Figure 4: PDFs for 2019 of t_{max} (a,d), t_{min} (b,e) and t_{mean} (c). Panels (a,b,c) identify the evaluation when compared to ERA5-Land and panels (d,e) identify the evaluation when compared to SCIA.

differences with the observational dataset exist (e.g., higher standard deviations characterise the SCIA t_{min} for 2019). Better performance in the models was found with respect to SCIA, with respect to σ , RHO and $RMSE$. The model that matches the reference model the closest is ICON, with a lower $RMSE$, a higher RHO and a σ that is close to the reference figure. With regard to 2020, capability measurement was also contaminated by differences in the observed dataset. Better performance when compared to ERA5-Land were found in the models, in terms of correlations, which increased to approximately 91, 93 and 97% in COSMO, WRF

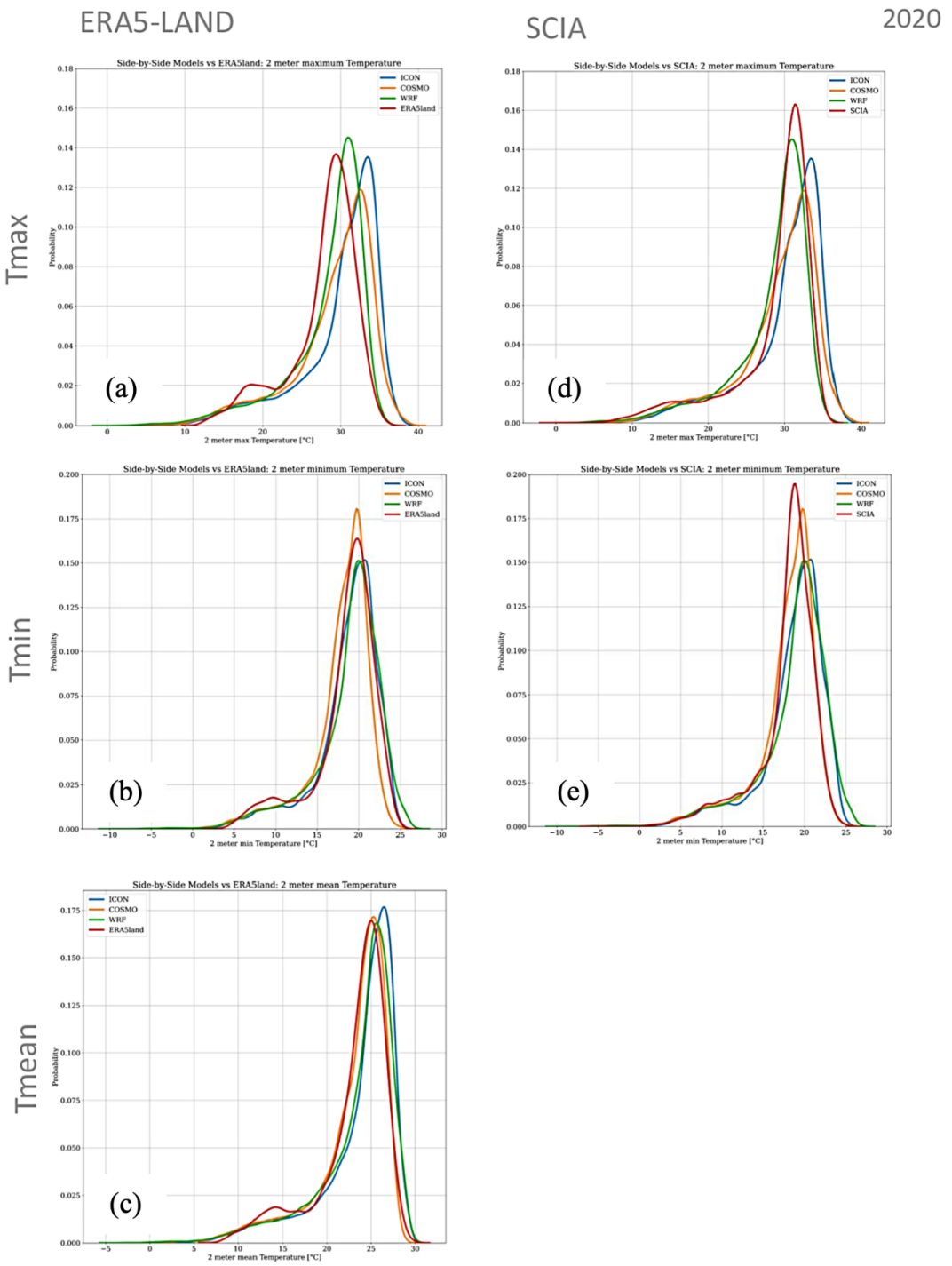

Figure 5: PDFs for 2020 of t_{max} (a,d), t_{min} (b,e) and t_{mean} (c). Panels (a,b,c) identify the evaluation against ERA5-Land and panels (d,e) identify the evaluation against SCIA.

and ICON respectively. Here, the latter model better simulates the t_{min} for 2020 when compared to the others.

The Taylor Diagram for t_{mean} are shown in Fig. 6 (i) and (l). High correlations between the reference model and the other models were found for 2019 (Fig. 6 (i)) and for 2020 (Fig. 6 l), with an $RMSE$ below 0.45°C and σ close to the observed model. Comparable performances (for the t_{mean} simulation) were found in the models.

Although there are slight differences between the two observational datasets, which in turn lead to differences in the capabilities of the models, WRF, ICON and COSMO revealed excellent performances in reproducing the temperature fields in the reference periods. Investigations into the

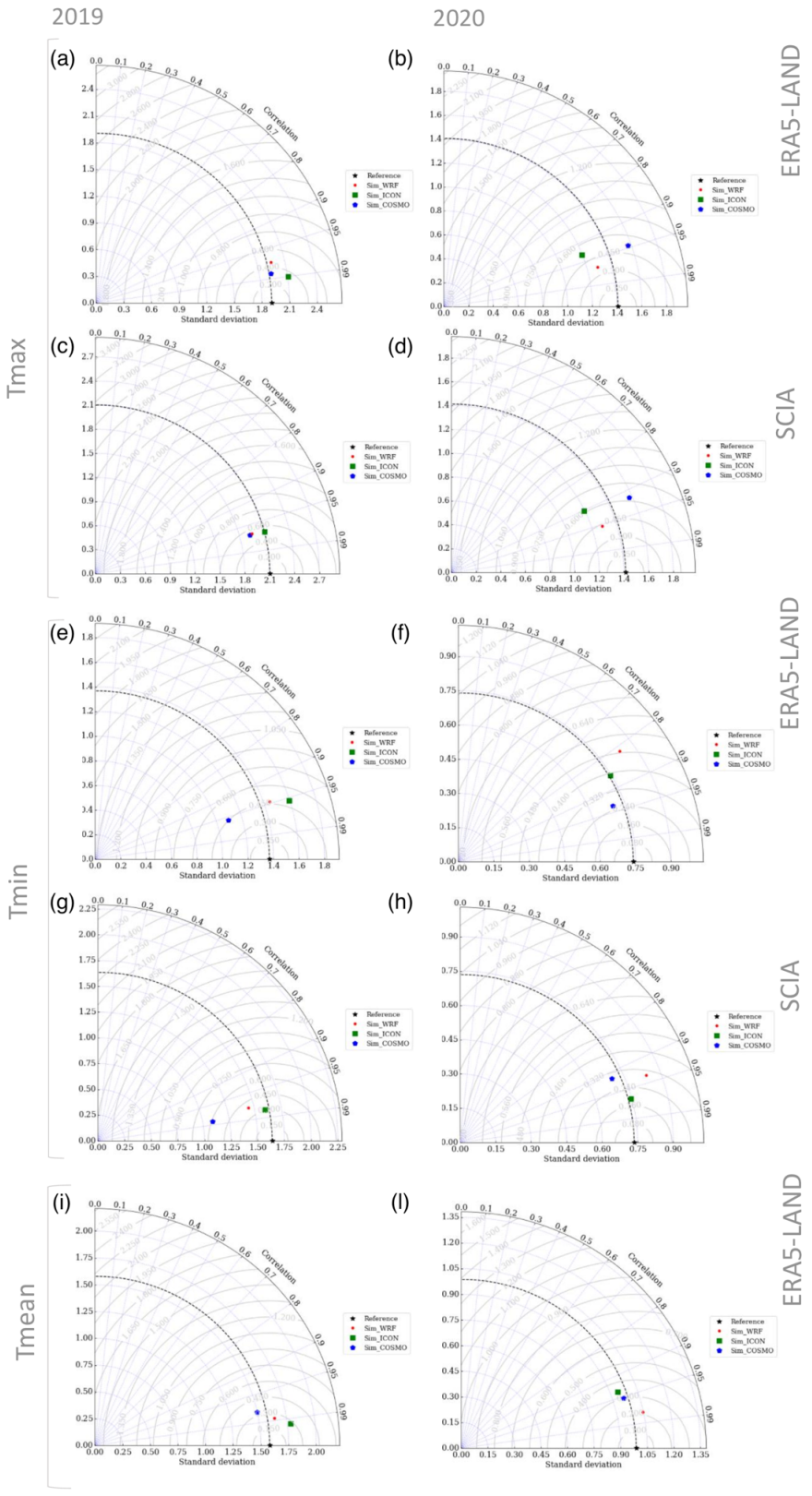

Figure 6: Taylor Diagrams for 2019 (left column) and 2020 (right column) of t_{max} (a,b,c,d), t_{min} (e,f,g,h) and t_{mean} (i,l). Panels (a,b,e,f,i,l) identify ERA5-Land, while the panels (c,d,g,h) identify SCIA.

differences between the two observational datasets will be left for future studies.

3.2 Precipitation

In this section we analyse the daily cumulative precipitation field produced by the three models at a 2 km-resolution and in comparison with the datasets ERA5-Land, at a resolution of 9 km, and SCIA, whose resolution for this variable is 10 km. In Fig. 7 the precipitation maps averaged in the reference periods are shown.

When comparing the two observational datasets in both the reference periods, differences between precipitation patterns are found: for 2019 (Fig. 7 a, b) SCIA captures heavier precipitation over Calabria, Molise, Abruzzo and Sicily when compared to ERA5-Land.

When comparing Fig. 7 (a) and (b) with the models maps for the same period, the models show patterns consistent with SCIA (Fig. 6 b). In fact, they accurately reproduce rain intensity over the region of Calabria, and in southern Italy. The weak precipitation spots found over the Alps and Sardinia are also captured by the models. However, it should be noted that WRF (Fig. 6 c) underestimates the Tot_{prec} when compared to observations made for in Central Italy, while COSMO and ICON accurately reproduce both the patterns and precipitation rate (Fig. 7 d, e). While analysing the precipitation patterns over the Puglia region, the capability of WRF is highly dependent on the reference dataset. In this respect, WRF accurately estimates the range of precipitation values captured by ERA5-Land, while it underestimates the Tot_{prec} values that characterise SCIA.

The same analysis over the 2020 reference period (Fig. 7 f,g,h,i,l) highlights effective model capabilities s in terms of reproducing the location of precipitation cores over Northern Italy, with differences along the Northern-Central Apennines. These differences also characterise the two-observational datasets, in fact ERA5-Land underestimates precipitation over the Alps when compared to SCIA and does not reproduce any precipitation cluster over the Central Apennines. The second half of August is characterised by intense storm systems that affect Italy, especially in numerous specific locations in Northern Italy during the journeys of unstable lines that creep across the country, with most coming from the Atlantic. In order to assess the capabilities of the model in terms of reproducing the meteorological conditions on the Italian Peninsula caused by this specific synoptic condition, SCIA has been taken as a reference, since it derives from station measurements. In this respect, WRF accurately estimates precipitation range with regard to values and main patterns, although slightly overestimating precipitation in the Alps. In contrast, COSMO accurately simulates precipitation distribution in the Alps sector (strongly underestimating the rain rate), however it is unable to simulate the precipitation cores over the Apennines. ICON, however, effectively captures the Tot_{prec} values and variability patterns on the Italian Peninsula, while slightly underestimating the rain rates over the North-Western Alps and on the Central Apennines.

In addition to the mean-precipitation maps, as with the temperature field, we analysed the PDFs for the Tot_{prec} variable in order to emphasise the differences between the models and the observations (Fig. 8).

Fig. 8 highlights a clear overestimation of the events without precipitations over Italy in both reference periods and both observational datasets, and this is balanced by a higher number of events with precipitations of over 15 mm per day. The model that more accurately resembles the observations for 2019 is COSMO, which estimates a PDF that is very close to the observed examples, however it simulates a restricted number of precipitation events with precipitations of over 10 mm per day, which is the maximum precipitation rate captured by ERA5-Land and SCIA (Fig. 8 a, b). The WRF model meanwhile effectively represents the observed precipitation PDF for 2020, matching the distribution for low precipitation values, however it tends to overestimate events with rainfall that is higher than 20 mm per day. In contrast, ICON and COSMO overestimate the number of events without precipitation over Italy but accurately capture the range of precipitation values (Fig. 8 c, d).

As with the temperature variable, the Taylor diagrams for simulated precipitation in WRF, COSMO and ICON that were evaluated against SCIA and ERA5-Land are discussed below.

Fig. 9 shows the differences between SCIA and ERA5-Land for both reference periods and that in turn provoke changes in the models' performances. The models agree more closely with SCIA, which has higher standard deviation than ERA5-Land. This suggests that the variability that is not captured by ERA5-Land and that is however present in SCIA, is simulated by the models.

For 2019, COSMO more accurately represents both the observed $RMSE$ value (0.43 mm/day) and RHO (0.93 mm/day) when compared to SCIA (Fig. 9 a, b), while in terms of σ WRF has a slightly better performance. Nonetheless, when evaluating the models against ERA5-Land, WRF has the most efficient performance for each of the three indicators, in fact the $RMSE$ value is smaller than the other two models (about 0.9 mm compared to 1.22 and 1.26 mm for COSMO and ICON respectively) and the σ is closer to the observed figure. In terms of correlation, the models do not accurately represent the precipitation variability during the reference period, in fact the most accurate among them is WRF, with a correlation of approximately 53%.

With respect to 2020, the WRF model more accurately simulates the precipitation variability observed in SCIA, with a similar standard deviation and a lower $RMSE$ when compared to the other models (Fig. 9 c, d). However, in terms of correlation, each model is able to reproduce the observed variability, reaching correlations of around 97%. When evaluating the models with ERA5-Land, WRF, COSMO and

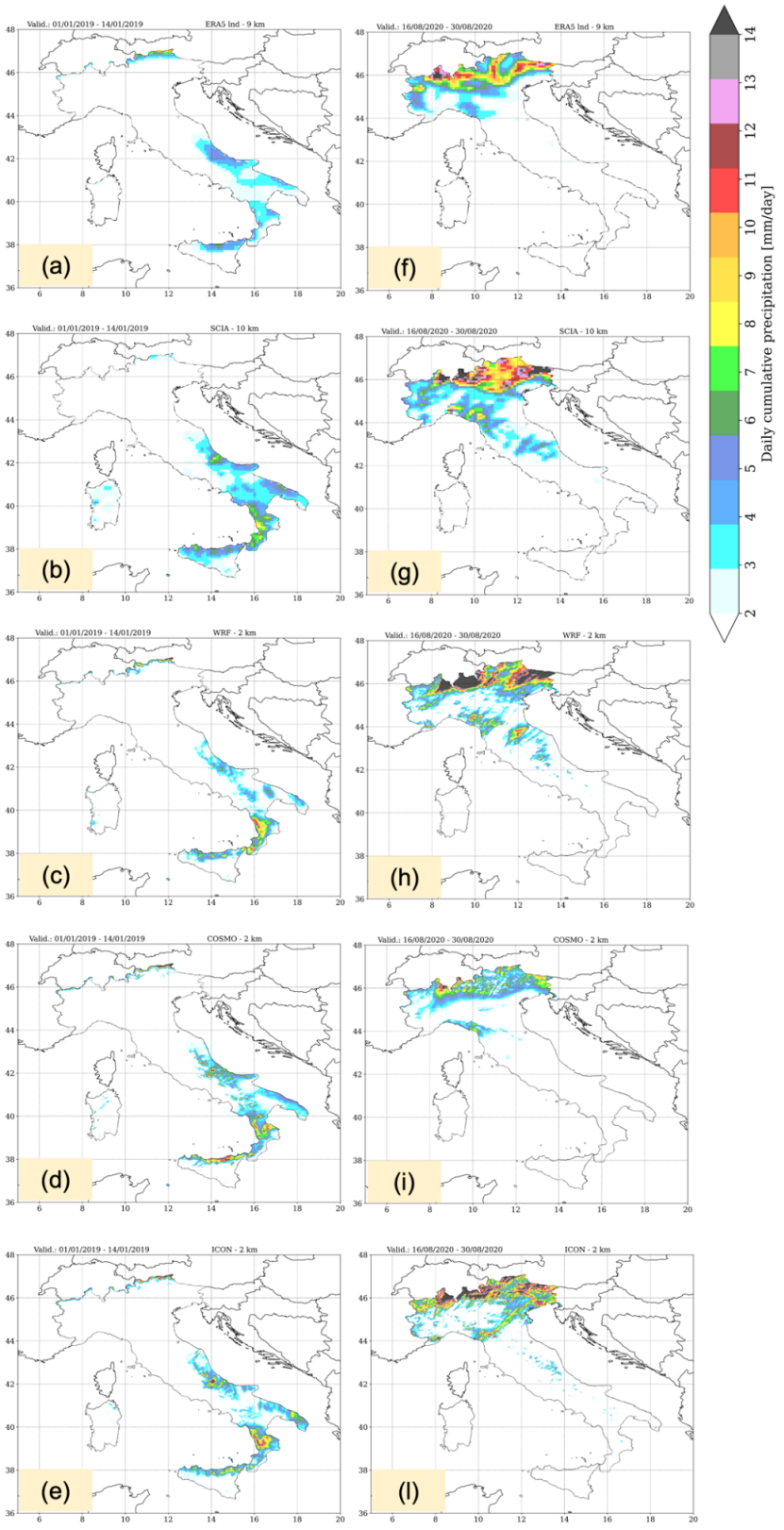

Figure 7: Map of Time-mean Daily Cumulative Precipitation at 2 m for ERA5-Land (a,f), SCIA (b,g), WRF (c,h), COSMO (d,i) and ICON (e,l).

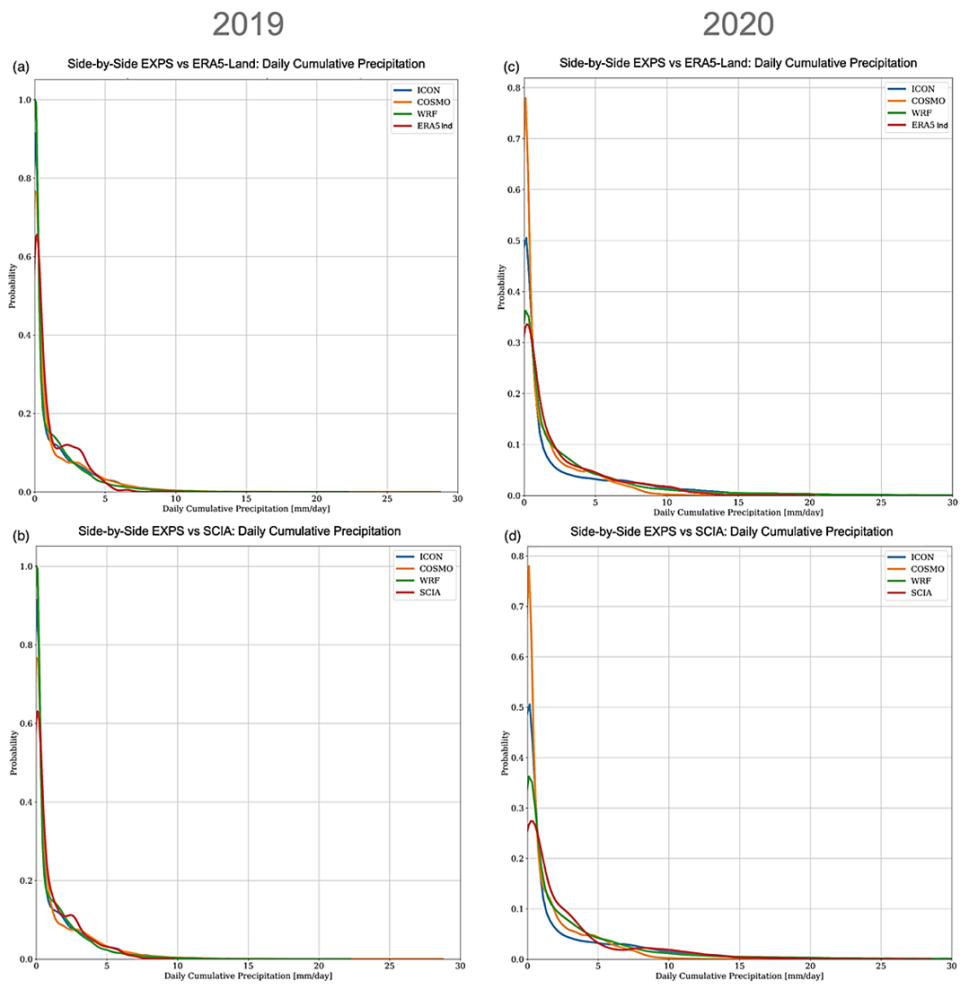

Figure 8: PDFs for Daily Cumulative Precipitation at 2 m in WRF, COSMO and ICON, when evaluated against ERA5-Land (a,c) and SCIA (b,d) in 2019 (left column) and 2020 (right column).

ICON all have similar skills in terms of $RMSE \approx 2.1\ mm$ and $RHO \approx 82\%$, however in terms of standard deviation ICON is the model with results closest to the observed data.

3.3 Wind

In order to validate the simulated mean wind speed data in the reference period for both models with respect to ERA5-Land (at a 9 km resolution) the same diagnostics for the temperature and precipitation fields were used. The time series of wind speed were selected at the level whose height is closest to 10 metres. Since they were originally at hourly resolution, values were aggregated into daily means for both reanalysis and model data. The first half of January 2019 was characterised by a wide trough, which extended from the Scandinavian Peninsula to the central Mediterranean basins, and by a strong positive anomaly at 500 hPa over the mid-Atlantic. This synoptic configuration leads to cold Arctic advection towards the Italian Peninsula with very cold temperatures over most of the national area. Strong winds were registered in Central and Southern Italy, and these probably corresponded to jet streams that could have been the cause of a deepening in the low pressure system and the strengthening of surface wind speeds. The overall quality validation results are inferred from the maps for 2019 (Fig. 10 a,b,c,d) and 2020 (Fig. 10 e,f,g,h). As with the other fields explored, resolution-based differences are also induced with respect to mean wind speed, resulting in the capability of the models to improve their simulation of W_{10m} variability at a finer scale. In order to create a robust standard with which to improve the performance comparison of the models, the results inferred here will be detailed in accordance with the Beaufort scale (World Meteorological Organization, 1970). In general terms, it can be observed that the bias of WRF, COSMO and ICON overestimate wind speed when compared to the reanalysis dataset for both 2019 and 2020, over the entire specific domain, with peaks being recorded from the models over 30 km/h (fresh breeze) for the winter and up to 24 km/h (moderate breeze) for summer, in comparison with the values observed in ERA5-Land, i.e. up to 24 km/h (moderate breeze) and 18 km/h (gentle breeze), respectively.

The patterns that emerge from the models are consistent

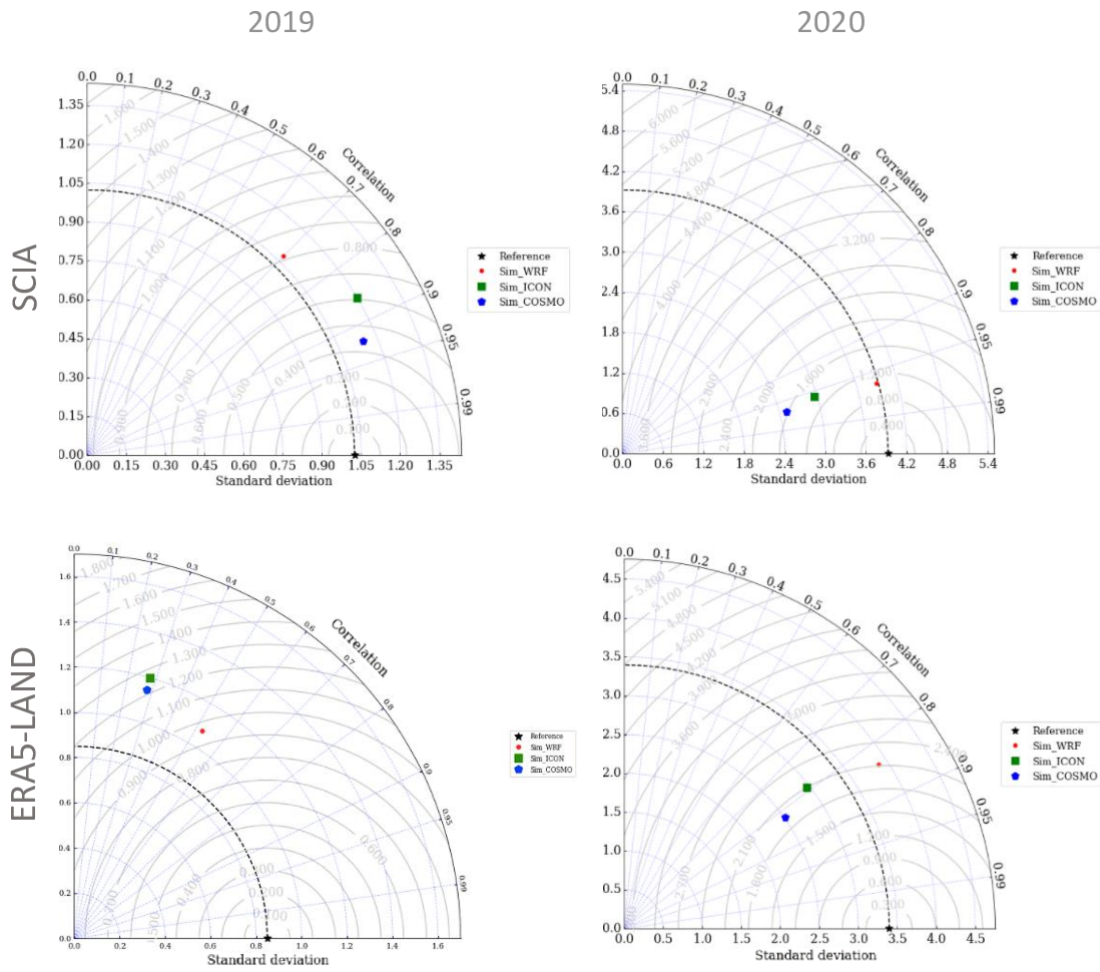

Figure 9: Taylor Diagrams of Daily Cumulative Precipitation at 2 m in WRF, COSMO and ICON when evaluated against ERA5-Land (a,c) and SCIA (b,d) in 2019 (left column) and 2020 (right column).

with each other for the entire Italian Peninsula, especially in terms of the signals registered between the provinces of Rome and Viterbo and for Reggio-Calabria during winter. All models reproduce higher values captured by the ERA5-Land in Foggia, 26 to 28 km/h and 22 to 24 km/h, respectively. For 2019, the overestimation appears less severe in fields reproduced by WRF and ICON in Alpine regions. In summer, the models tend to overestimate W_{10m} on the Italian Peninsula (especially with respect to WRF in the Central Apennines), except for the Region of Calabria, where the models underestimate wind speed. Furthermore WRF provided better simulations for higher wind speed values in North-Eastern Sardinia 16 to 18 km/h, than those reproduced by the reanalysis (Fig. 10 e, f).

Further quantitative assertions are made below, using PDF and Taylor diagrams. In Fig. 11, shows that the highest probability value is associated to $\sim$5 km/h for the models and for ERA5-Land, whose distribution is narrower than that of the models, and which describes a lower variability. The PDF for the WRF model is a better match for the PDF in terms of the reanalysis, with two peaks at around 5 km/h and 10 km/h, in contrast to those found in ICON and COSMO. While COSMO clearly overestimates these values, with speeds reaching around 50 km/h (near gale), and which were probably pertinent to the Alpine areas, as mentioned previously. In summer (Fig. 11 b) the highest probability is similar for COSMO, ICON and ERA5-Land, especially the shape of the PDF in ICON is close to the reanalysis one, while WRF model describes a stronger variability, simulating higher values in the wind speed field.

The Taylor diagrams shown in Fig. 12 are discussed here. Higher values of RMSE are found in WRF when compared to ICON and COSMO in both 2019 and 2020 (2.2 km/h and 1.6 km/h, respectively). Furthermore, stronger correlations with the reanalysis were found in the ICON model, when compared to the others (0.5 for winter and 0.7 for summer). All models capture greater variability than ERA5-Land (approximately 1.8) in winter, with a standard deviation between 1.8 and 2.1, while in the summer period only WRF records a more accentuated variability (1.8) with respect to the other models and the reanalysis, and which is characterised by a value of around 1.4.

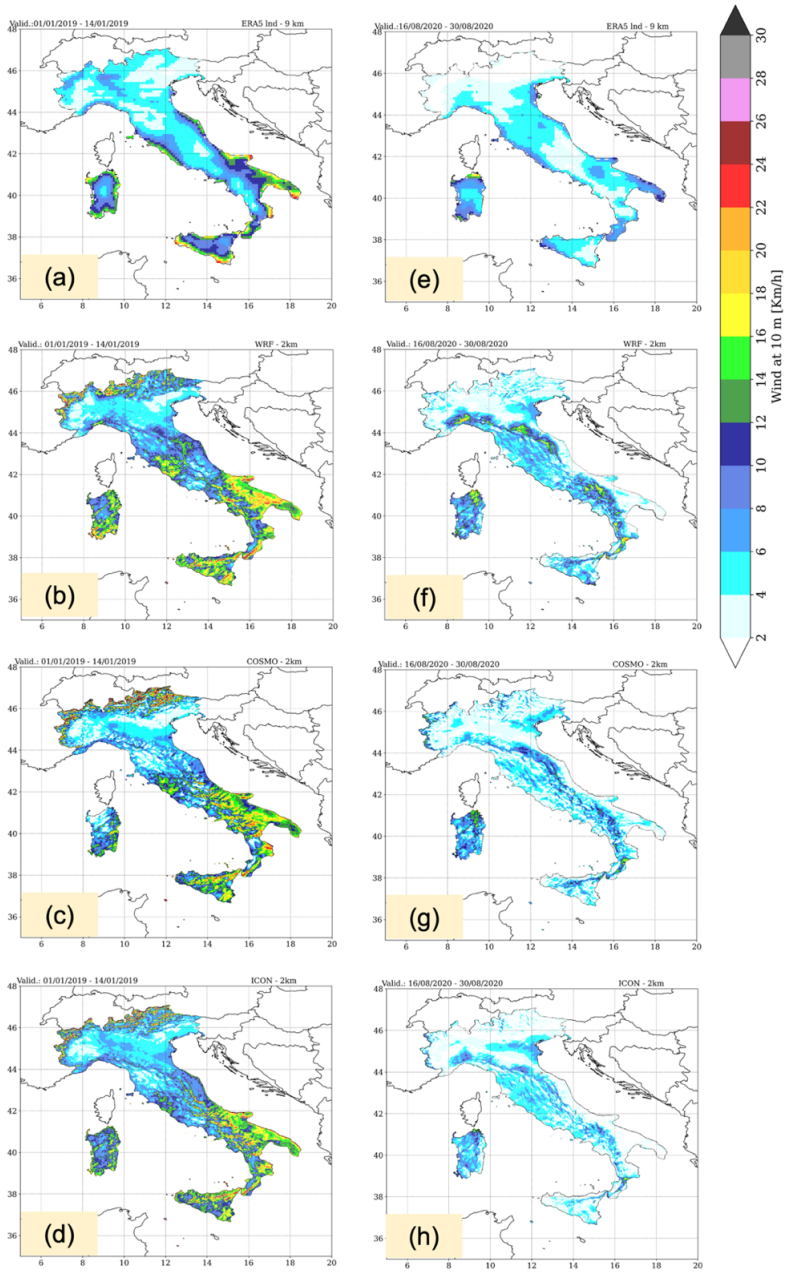

Figure 10: Map of Time-mean Wind Speed at 10 m for ERA5-Land (a,e), WRF (b,f), COSMO (c,g) and ICON (d,h).

4 Discussion and Conclusions

The main aim of this study is to evaluate the ability of three LAM models to simulate atmospheric short-term variability over the Italian Peninsula during two reference periods: from 01/01/2019 to 15/01/2019 and from 16/08/2020 to 30/08/2020. A preliminary study was conducted on each model in order to select the respective optimum configurations by means of a sensitivity analysis that allowed the evaluation of each model's performance in terms of computational efficiency and parallel communication. In the first case, the faster model in terms of single day simulation is ICON, while COSMO possesses more efficient communication between the nodes in parallel.

After this first step, we focused on the ability of the three models to reproduce three atmospheric variables: temperature, precipitation and wind speed over the entire domain, while evaluating the models' outputs against two observational datasets: SCIA and ERA5-Land.

The results for each model show that the variables analysed in this study are all consistent with regard to those observed. In this respect the models were shown to simulate values in a similar range, while reproducing patterns that were placed in the same geographic areas. Their short-term changes were also well captured: the temperature

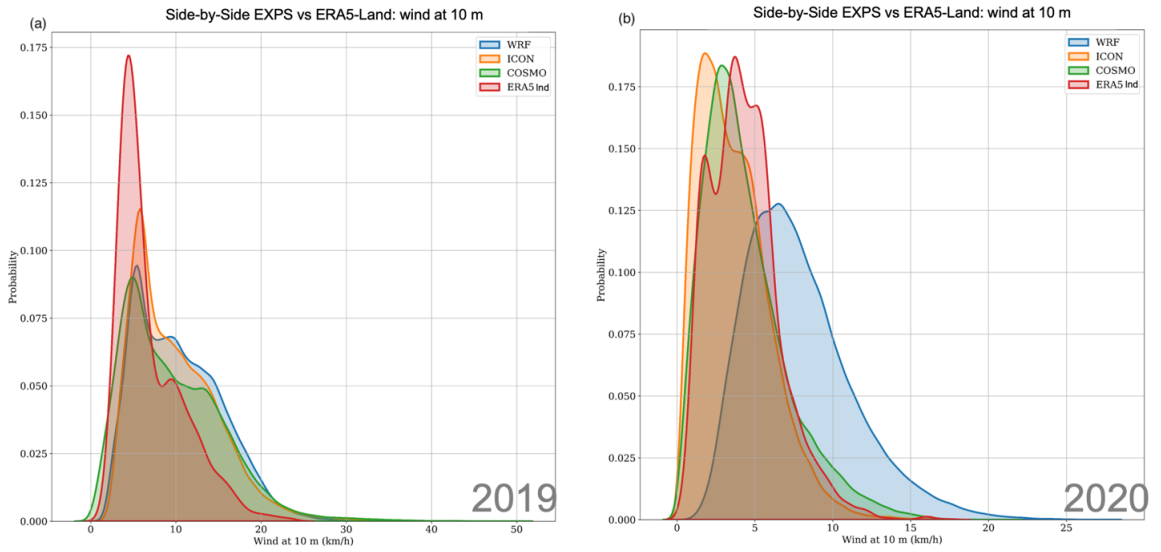

Figure 11: PDFs for Wind Speed at 10 m in WRF, COSMO and ICON when evaluated against ERA5-Land for 2019 (left) and 2020 (right).

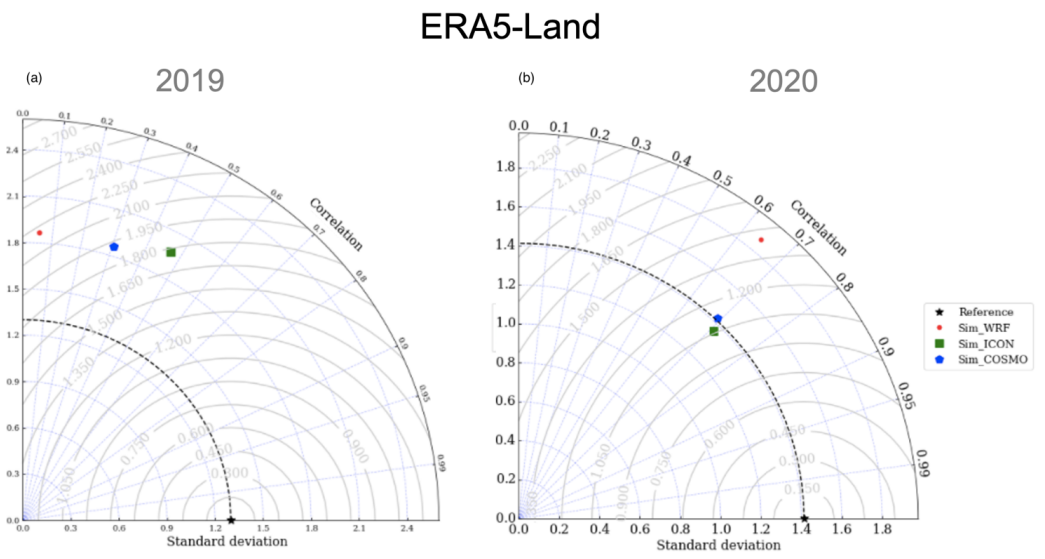

Figure 12: Taylor Diagrams for Wind speed at 10 m in WRF, COSMO and ICON when evaluated against ERA5-Land for 2019 (left) and 2020 (right).

reached high correlation values, extending between 80 to 99% (t_{max}: 93 to 99% and 90 to 97% in ERA5-Land and SCIA respectively. t_{min}: 81 to 96% and 91 to 99% in ERA5-Land and SCIA respectively. t_{mean}: 94 to 99% in ERA5-Land). Moreover low $RMSE$ and standard deviations closer to those observed were found, which highlighted excellent performances in reproducing the temperature fields in the reference periods and domains for each model. The precipitation field is well simulated by the models, when evaluated against SCIA, reaching values of 70 to 96%, with standard deviations comparable to those observed and minor $RMSE$ values. When comparing the models with ERA5-Land, the impact of the coarser resolution emerges. In fact, in terms of precipitation and wind speed, the coarser resolution of ERA5-LAND could affect their reproducibility and not allow them to resolve dynamic processes at finer scales that WRF, COSMO and ICON however, are able to capture. In conclusion, all models were able to properly capture the specific weather conditions, with cold temperatures and strong winds during winter and intense convection in summer, with differences between the models and the reference datasets, due to different horizontal resolutions. Furthermore, differences among the models may be related to the choice of more or less complex parameterizations in WRF, COSMO, and ICON, especially with respect to microphysics, PBL, and long and short wave radiations, that could affect the different ability of the models to capture the prevailing wind patterns and the precipitation nuclei in terms of both the intensity and the location of the latter.

Acknowledgments

ERA5-Land was produced with funding from the European Union's Copernicus Climate Change Service. The authors would like to thank the national and regional Italian agencies that contributed to providing the SCIA system (www.scia.isprambiente.it, accessed on 3 December 2021) with the data used in this research. The authors would also like to thank the atmospheric numerical model development community for its enormous ongoing efforts in the implementation and continued updating of the NWP models COSMO (v.5.05), ICON (v.2.6.2.2) and the WRF (v.4.2.1) models. The entire simulation work was performed using the calculation resources of the REMHI (Regional Models and geo-Hydrological Impacts) division of the CMCC (Euro-Mediterranean Centre on Climate Change) Foundation.

Data Availability Statement

ERA5-Land data is freely available on the Copernicus Climate Change Service (C3S) web platform (https://climate.copernicus.eu/), while the SCIA data may be obtained free at http://www.scia.isprambiente.it/wwwrootscia/help_eng.html.

Appendix A

The preliminary sensitivity analysis that was performed on WRF and ICON models in order to define their best configurations, are detailed in the tables A1 and A2. As mentioned in Section 2.1.2, the sensitivity analysis conducted by Garbero et al. (2021) provides the configuration for the COSMO model.

References

Baldauf, M., Seifert, A., Förstner, J., Majewski, D., Raschendorfer, M., and Reinhardt, T., 2011: *Operational convective-scale numerical weather prediction with the COSMO model: Description and sensitivities*, Mon. Weather Rev., **139**, 3887–3905.

Buzzi, M.: Challenges in operational numerical weather prediction at high resolution in complex terrain, Ph.D. thesis, ETH Zurich, 2008.

Caldas-Alvarez, A., Augenstein, M., Ayzel, G., Barfus, K., Cherian, R., Dillenardt, L., Fauer, F., Feldmann, H., Heistermann, M., Karwat, A., et al., 2022: *Meteorological, impact and climate perspectives of the 29 June 2017 heavy precipitation event in the Berlin metropolitan area*, Nat. Hazards Earth Syst. Sci., **22**, 3701–3724.

De Lucia, C., Bucchignani, E., Mastellone, A., Adinolfi, M., Montesarchio, M., Cinquegrana, D., Mercogliano, P., and Schiano, P., 2022: *A Sensitivity Study on High Resolution NWP ICON—LAM Model over Italy*, Atmosphere, **13**, 540.

Desiato, F., Lena, F., and Toreti, A., 2007: *SCIA: a system for a better knowledge of the Italian climate*, Bollettino di Geofisica Teorica ed Applicata, **48**, 351–358.

Doms, G., Förstner, J., Heise, E., Herzog, H., Mironov, D., Raschendorfer, M., Reinhardt, T., Ritter, B., Schrodin, R., Schulz, J.-P., et al., 2011: *A description of the nonhydrostatic regional COSMO model. Part II: Physical parameterization*, Deutscher Wetterdienst.

Garbero, V., Milelli, M., Bucchignani, E., Mercogliano, P., Varentsov, M., Rozinkina, I., Rivin, G., Blinov, D., Wouters, H., Schulz, J.-P., et al., 2021: *Evaluating the urban canopy scheme TERRA_URB in the COSMO model for selected European cities*, Atmosphere, **12**, 237.

Heppelmann, T., Steiner, A., and Vogt, S., 2017: *Application of numerical weather prediction in wind power forecasting: Assessment of the diurnal cycle*, Meteorol. Z., **10**.

Kim, S., Matsuura, T., Matsumi, Y., Kazuhisa, T., Yasuda, T., Tom, T., and Mase, H., 2013: *Effects of WRF parameterization on meteorological predictions in the mid-latitude region-planetary boundary layer scheme and cloud microphysics*, J. Jpn. Soc. Civil Eng., **2**.

Laprise, R., 1992: *The Euler equations of motion with hydrostatic pressure as an independent variable*, Mon. Weather Rev., **120**, 197–207.

Mugume, I., Basalirwa, C., Waiswa, D., Nsabagwa, M., Ngailo, T. J., Reuder, J., Semujju, M., et al., 2018: *A comparative analysis of the performance of COSMO and WRF models in quantitative rainfall prediction*, Int. J. Mar. Sci., **12**, 130–138.

Mulovhedzi, P. T., Rambuwani, G. T., Bopape, M.-J., Maisha, R., and Monama, N., 2021: *Model inter-comparison for short-range forecasts over the southern African domain*, S. Afr. J. Sci., **117**, 1–12.

Muñoz-Sabater, J., Dutra, E., Agustí-Panareda, A., Albergel, C., Arduini, G., Balsamo, G., Boussetta, S., Choulga, M., Harrigan, S., Hersbach, H., et al., 2021: *ERA5-Land: A state-of-the-art global reanalysis dataset for land applications*, ESSD, **13**, 4349–4383.

Muñoz Sabater, J. et al., 2019: *ERA5-Land hourly data from 1981 to present*, Copernicus Climate Change Service (C3S) Climate Data Store (CDS), **10**.

Park, S.-H., Klemp, J. B., and Kim, J.-H., 2019: *Hybrid mass coordinate in WRF-ARW and its impact on upper-level turbulence forecasting*, Mon. Weather Rev., **147**, 971–985.

Schättler, U., Doms, G., and Schraff, C., 2018: *A Description of the Nonhydrostatic Regional COSMO-Model. Part VII: User's Guide*, Deutscher Wetterdienst, **226**.

Schulz, J.-P., Vogel, G., Becker, C., Kothe, S., and Ahrens, B., 2015: *Evaluation of the ground heat flux simulated by a multi-layer land surface scheme using high-quality observations at grass land and bare soil*, in: EGU conference abstracts, p. 6549.

Silvestri, L., Saraceni, M., and Bongioannini Cerlini, P., 2022: *Links between precipitation, circulation weather types and orography in central Italy*, Int. J. Climatol., **42**, 5807–5825.

Skamarock, W. C., Klemp, J. B., Dudhia, J., Gill, D. O., Liu, Z., Berner, J., Wang, W., Powers, J., Duda, M., Barker, D., et al., 2019: *A description of the advanced research WRF version 4*, NCAR tech. note, **145**.

Steppeler, J., Doms, G., Schättler, U., Bitzer, H., Gassmann, A., Damrath, U., and Gregoric, G., 2003: *Meso-gamma scale forecasts using the nonhydrostatic model LM*, Meteorol. Atmos. Phys., **82**, 75–96.

World Meteorological Organization, 1970: The Beaufort Scale of Wind Force. Technical and Operational Aspects, 3, WMO. Commission for Maritime Meteorology.

Wouters, H., Demuzere, M., De Ridder, K., and van Lipzig, N. P., 2015: *The impact of impervious water-storage parametrization on urban climate modelling*, Urban Climate, **11**, 24–50.

Wouters, H., Demuzere, M., Blahak, U., Fortuniak, K., Maiheu, B., Camps, J., Tielemans, D., and van Lipzig, N. P., 2016: *The efficient urban canopy dependency parametrization (SURY) v1. 0 for atmospheric modelling: description and application with the COSMO-CLM model for a Belgian summer*, Geosci. Model Dev., **9**, 3027–3054.

Zängl, G., Reinert, D., Rípodas, P., and Baldauf, M., 2015: *The ICON (ICOsahedral Non-hydrostatic) modelling framework of DWD and MPI-M: Description of the non-hydrostatic dynamical core*, Q. J. R. Meteorol., **141**, 563–579.

Table A1: The sensitivity analysis on PBL, microphysics, surface physics schemes and geographic projection allowed the determination of the best WRF configuration, while minimising the error metrics for precipitation, wind speed and temperature fields (Sim 9).

Sensitivity Group	Planetary Boundary Layer Scheme	Deep Convection Scheme	Microphysics Scheme	Land Surface Scheme	Map Projections
ref	Mellor	no cumulus parameterization	Thompson graupel	unified Noah land-surface model	Mercator
Sim 1	Mellor	no cumulus parameterization	Thompson graupel	unified Noah land-surface model	Conformal Lambert
Sim 2	Mellor	Tiedtke	Thompson graupel	unified Noah land-surface model	Conformal Lambert
Sim 3	Mellor	no cumulus parameterization	Thompson graupel	thermal diffusion	Conformal Lambert
Sim 4	Mellor	no cumulus parameterization	WSM 6-class graupel	thermal diffusion	Conformal Lambert
Sim 5	Mellor	no cumulus parameterization	Morrison 2-moment	thermal diffusion	Conformal Lambert
Sim 6	Mellor	no cumulus parameterization	NSSL 2-moment 4-ice	thermal diffusion	Conformal Lambert
Sim 7	YSU	no cumulus parameterization	Thompson graupel	thermal diffusion	Conformal Lambert
Sim 8	YSU	no cumulus parameterization	WSM 6-class graupel	thermal diffusion	Conformal Lambert
Sim 9	YSU	no cumulus parameterization	Morrison 2-moment	thermal diffusion	Conformal Lambert
Sim 10	YSU	no cumulus parameterization	NSSL 2-moment 4-ice	thermal diffusion	Conformal Lambert

Table A2: The Parameterization Schemes available in ICON, modified in the Sensitivity Analysis. The rows indicate the configurations of each simulation. Sim9 is the configuration that best reduces errors with respect to the observed data (De Lucia et al., 2022).

Sensitivity Group	Shallow Conv	Radiation Scheme	Cloud Microphysics	Cloud Cover	Turbulent Transfer
ref	TRUE	ecRad	microphysics, 3-cat ice: cloud ice, snow, graupel	diagnostic cloud cover (Koehler)	COSMO diffusion and transfer
Sim 1	FALSE	ecRad	microphysics, 3-cat ice: cloud ice, snow, graupel	diagnostic cloud cover (Koehler)	COSMO diffusion and transfer
Sim 2	TRUE	RRTM	microphysics, 3-cat ice: cloud ice, snow, graupel	diagnostic cloud cover (Koehler)	COSMO diffusion and transfer
Sim 3	TRUE	Ritter-Geleyn radiation	microphysics, 3-cat ice: cloud ice, snow, graupel	diagnostic cloud cover (Koehler)	COSMO diffusion and transfer
Sim 4	TRUE	PSRAD	microphysics, 3-cat ice: cloud ice, snow, graupel	diagnostic cloud cover (Koehler)	COSMO diffusion and transfer
Sim 5	TRUE	ecRad	Two-moment microphysics (Seifert)	diagnostic cloud cover (Koehler)	COSMO diffusion and transfer
Sim 6	TRUE	ecRad	Koehler scheme with improved ice nucleation	diagnostic cloud cover (Koehler)	COSMO diffusion and transfer
Sim 7	TRUE	ecRad	Kessler scheme	diagnostic cloud cover (Koehler)	COSMO diffusion and transfer
Sim 8	TRUE	ecRad	microphysics, 3-cat ice: cloud ice, snow, graupel	COSMO SGS cloud scheme	COSMO diffusion and transfer
Sim 9	TRUE	ecRad	microphysics, 3-cat ice: cloud ice, snow, graupel	clouds as in turbulence (turbdiff)	COSMO diffusion and transfer
Sim 10	TRUE	ecRad	microphysics, 3-cat ice: cloud ice, snow, graupel	grid scale clouds	COSMO diffusion and transfer
Sim 11	TRUE	ecRad	microphysics, 3-cat ice: cloud ice, snow, graupel	diagnostic cloud cover (Koehler)	GME turbulence scheme
Sim 12	TRUE	ecRad	microphysics, 3-cat ice: cloud ice, snow, graupel	diagnostic cloud cover (Koehler)	Classical Smagorinsky diffusion